Quantum Information Processing (2021) 20:289
https://doi.org/10.1007/s11128-021-03232-8

Impact of graph structures for QAOA on MaxCut

Rebekah Herrman[1] · Lorna Treffert[1] · James Ostrowski[1] · Phillip C. Lotshaw[2] · Travis S. Humble[2] · George Siopsis[3]

Received: 31 March 2021 / Accepted: 18 August 2021 / Published online: 1 September 2021

Abstract

The quantum approximate optimization algorithm (QAOA) is a promising method of solving combinatorial optimization problems using quantum computing. QAOA on the MaxCut problem has been studied extensively on graphs with specific structure; however, little is known about the general performance of the algorithm on arbitrary graphs. In this paper, we investigate how different graph characteristics correlate with QAOA performance at depths at most three on the MaxCut problem for all connected non-isomorphic graphs with at most eight vertices. Some good predictors of QAOA success relate to graph symmetries, odd cycles, and density. For example, on eight vertex graphs, the average probability for selecting an optimal solution for graphs that contain no odd cycles after three iterations of QAOA is 60.6% compared to 48.2% for those that do. The data generated from these studies are shared in a publicly accessible database to serve as a benchmark for QAOA calculations and experiments. Knowing the relationship between structure and performance can be used to identify classes of combinatorial problems that are likely to exhibit a quantum advantage.

Keywords QAOA · Graph structures · MaxCut · Correlation

✉ Rebekah Herrman
rherrma2@tennessee.edu

James Ostrowski
jostrows@tennessee.edu

George Siopsis
siopsis@tennessee.edu

[1] Department of Industrial and Systems Engineering, The University of Tennessee, Knoxville, TN 37996-2315, USA

[2] Oak Ridge National Laboratory, Quantum Computing Institute, Oak Ridge, TN 37830, USA

[3] Department of Physics and Astronomy, The University of Tennessee, Knoxville, TN 37996-1200, USA

1 Introduction

Quantum computing has been shown to provide a theoretical advantage over classical computing in different areas such as machine learning and algorithms on shallow circuits [1,2], and noisy intermediate-scale quantum (NISQ) devices provide an opportunity to test this advantage. The quantum approximate optimization algorithm (QAOA) is a promising application of NISQ devices developed by Farhi, Goldstone, and Gutmann to solve combinatorial optimization (CO) problems [3]. Large-scale testing of QAOA has been difficult, as the size of problems that can be tested on NISQ hardware is limited and quantum simulations can be time-consuming for small problems. Thus, the current literature has mostly focused on examining graphs with a predetermined structure [4].

The impact of problem structure on computational efficiency is well understood in optimization community [5]: it is common for a difficult class of problems to become easy when a certain structure is imposed. By focusing on graphs with a predetermined structure in QAOA, there is a risk that conclusions made will not extend to the broader class of problems. In this paper, we seek to remedy this issue by performing an exhaustive analysis of how graph structure can impact QAOA on MaxCut problems, which have been the major focus of recent quantum computing research. We specifically examine connected graphs that have between three and eight vertices. The MaxCut problem on an undirected, simple graph $G = (V(G), E(G))$ is to determine how to partition $V(G)$ into two sets such that the number of edges between them is maximized. This problem is classically hard; however, heuristics exist that find near-optimal solutions [6,7].

QAOA for MaxCut has been studied on two and three regular graphs [3,8–11], and random regular bipartite graphs [4], which are families that are not representative of the vast majority of graphs. Other work has focused on more general graphs, for instance Erdős-Rényi random graphs [12], but over small samples. Additionally, some of the more commonly studied measure of QAOA success are the expected value of C, $\langle C \rangle$, and the approximation ratio [13], $\frac{\langle C \rangle}{C_{\max}}$, where $C_{\max}$ is the size of the cut in an optimal solution. Our goal is to look at general graphs and determine which structures correlate to better performances of QAOA on MaxCut for not only $\langle C \rangle$ and $\frac{\langle C \rangle}{C_{\max}}$ but also the probability of measuring an optimal solution, $P(C_{\max})$, and the change in the approximation ratio from level p QAOA to level $p + 1$.

To this end, we analyze graph structures and compare them to simulations of the algorithm on MaxCut at one, two, and three levels for all non-isomorphic, connected graphs on up to eight vertices. We then examine correlations between the graph properties and the metrics of QAOA success listed in the following section. A summary of the results is found in Table 2. Finally, we created a database containing all connected graphs on at most eight vertices and the structures that were examined. The details for accessing the database are found in Appendix 2.

This paper is organized as follows: First, we review MaxCut and QAOA in Sect. 2. In Sect. 3, we discuss graph characteristics and their correlations to QAOA performance metrics. We then summarize the results and discuss future work in Sect. 4.

2 QAOA and MaxCut background

In order to use QAOA to solve a CO problem, two operators, $U(C, \gamma) = e^{-iC\gamma}$ and $U(B, \beta) = e^{-iB\beta}$, are applied in succession on an initial state. Here, β and γ are angles that lie in the interval $[0, 2\pi)$. The initial state is denoted $|s\rangle$ and is often the uniform superposition, $|s\rangle = \frac{1}{\sqrt{2^n}} \sum_z |z\rangle$, where z refers to the computational basis states. QAOA applied p times to $|s\rangle$ is denoted p-QAOA. The combined operator for the p-QAOA is

$$|\gamma, \beta\rangle = U(B, \beta_p)U(C, \gamma_p)...U(B, \beta_1)U(C, \gamma_1)|s\rangle.$$

C encodes the problem to be solved and B is a mixing operator.

MaxCut is a CO problem that is relatively straightforward to encode and solve with QAOA. The goal of the MaxCut problem is to partition the vertices of a graph $G = (V(G), E(G))$ such that the number of edges that has an endpoint in each set is maximized. We identify each vertex of G with a qubit and let $C = \sum_{ij \in E(G)} C_{ij}$ and define

$$C_{ij} = 1/2(-\sigma_i^z \otimes \sigma_j^z + I),$$

where σ_i^z refers to the Pauli-z matrix acting on qubit i and I refers to the 2^n identity matrix. B is typically

$$B = \sum_{v \in V(G)} B_v.$$

In this case, $B_v = \sigma_v^x$ is the Pauli-x operator acting on the vth qubit. If B is chosen differently, $|s\rangle$ is chosen such that it is an eigenstate of B.

The expected value of C after p iterations is $\langle \gamma, \beta | C | \gamma, \beta \rangle$, which we denote as $\langle C \rangle_p$ or $\langle C \rangle$ when p is clear from context. The approximation ratio is one common metric of QAOA success is $\langle C \rangle / C_{\max}$, where $C_{\max}$ is the optimal solution to the CO problem.

3 Graph structures

In the previous work, we ran numerical simulations of QAOA solving the MaxCut problem on all non-isomorphic graphs with the number of vertices, n, ranging between three and eight [14]. The angles that maximize $\langle C \rangle$ after one iteration of QAOA were solved using the open-source software Couenne [15]. For larger p, we used the Broyden–Fletcher–Goldfarb–Shanno (BFGS) algorithm to find angles that maximize $\langle C \rangle$. The algorithm inputs an initial collection of angles and then uses a numerical gradient and second-order approximate Hessian to find angles that converge to local maxima of $\langle C \rangle$ [16]. The BFGS algorithm was used as a heuristic to determine optimized angles using hundreds of random seeds for each graph. We used 50 random-angle seeds when $p = 1$, 100 random seeds when $p = 2$, and 500 seeds when $p = 3$. The optimized results are consistent between different implementations and are confirmed to be global optimal solutions in small cases with $n \leq 6$ and $p = 2$ by comparing against a brute-force search. We ran BFGS calculations a second time on

Table 1 The number of connected, non-isomorphic graphs on n vertices for $3 \leq n \leq 8$

n	Number of connected, non-isomorphic graphs on n vertices, N_n
3	2
4	6
5	21
6	112
7	853
8	11117

all graphs with $n > 6$ for $p = 2$ and for all n with $p = 3$, using different sets of 100 or 500 random seeds in order to verify the results were consistent. Thus, the correlations we draw can be thought of as applying to "best-case" results for QAOA. The values of $\langle C \rangle$ and probabilities of measuring an optimal solution are compiled in a publicly accessible data set [17].

Using the numerical simulations from earlier work, we determine QAOA metrics of interest. The metrics used are:

- $\langle C \rangle$: The expected value of C
- $P(C_{\max})$: The probability of measuring a state that represents a maximum cut
- Level p approximation ratio: $\frac{\langle C \rangle_p}{C_{\max}}$
- Percent change in approximation ratio (Δ ratio) at p: $\frac{\frac{\langle C \rangle_p}{C_{\max}} - \frac{\langle C \rangle_{p-1}}{C_{\max}}}{1 - \frac{\langle C \rangle_{p-1}}{C_{\max}}} = \frac{\langle C \rangle_p - \langle C \rangle_{p-1}}{C_{\max} - \langle C \rangle_{p-1}}$.

$\langle C \rangle$ can be written as the sum of expected values for the operator acting on each edge in the graph, where each edge expectation value at p iterations depends on vertices up to p edges away, so more iterations of QAOA allow the algorithm to "see" more of the graph structure. The level p approximation ratio is the expected value of the cost function for MaxCut for QAOA performed at level p as a percentage of the optimal solution, and the Δ ratio tells us the rate of change of the level per iteration.

For three vertex graphs, QAOA was only run on two levels, as the correct solution was found with two iterations. Three iterations of QAOA were applied to graphs with $n \geq 4$. Table 1 lists the number of connected, non-isomorphic graphs on n vertices. As there are only two connected graphs on three vertices, the data for $n = 3$ do not give much insight into the correlations between the structures and different QAOA properties, so we exclude the data for three vertex graphs from all tables. We study only connected graphs because if the graph is disconnected, each component has fewer vertices, and we can independently solve each connected sub-problem. We also study non-isomorphic graphs, as isomorphic graphs have the same properties and result in the same solutions.

We collected properties of the tested graphs and found the Pearson's correlation coefficient between them and each metric. The properties examined were:

- Number of edges
- Diameter
- Clique number

Table 2 The trends in correlations between the group properties and each QAOA metric

Graph property	$\langle C \rangle$	$P(C_{\max})$	$\frac{\langle C \rangle_p}{C_{\max}}$	$\frac{\langle C \rangle_p - \langle C \rangle_{p-1}}{C_{\max} - \langle C \rangle_{p-1}}$
Edges	=	−	−	=
Diameter	=		−	=
Clique number	−	−	−	
Bipartite	−		−	
Eulerian	=		=	
Distance regular	=	=	=	
Number of cut vertices	=	=	+	=
Number of minimal odd cycles	−	−	−	−
Group size	=	=	=	
Number of orbits	=	−	−	−

The symbol "+" refers to correlations that tend to increase, "−" refers to a correlation that tend to decrease, and "=" refers to correlations that tend to stay constant for fixed n as p increases. An empty space refers to a property with no strong correlation or discernible trend

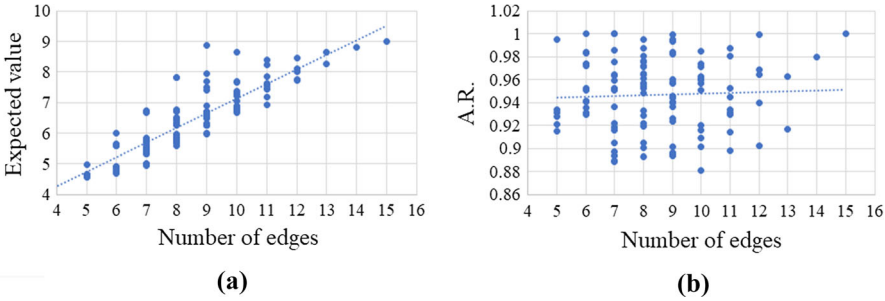

Fig. 1 $\langle C \rangle$ and the approximation ratio, denoted "A.R.", plotted against the total number of edges in the graph for $p = 3$. There is a strong positive correlation, with $r = .875$ in 2a and lack of correlation in 2b, with coefficient $r = .042$

- Number of cut vertices
- Number of minimal odd cycles
- Group size
- Number of orbits
- Bipartite (Boolean)
- Distance regularity (Boolean)
- Eulerian (Boolean)

Throughout the text and charts, r denotes the correlation coefficient and n denotes the number of vertices. Definitions of the graph theory terms are presented in Appendix 1. These properties are a subset of all the possible graph properties, but were chosen because they are commonly studied. We are providing the database to enable others to identify other structures of interest. The tables listing correlation coefficients are found in Appendix 3. The graphs and numbering system are from the connected graph files by Brendan McKay [18]. In the following subsections, we discuss graph properties

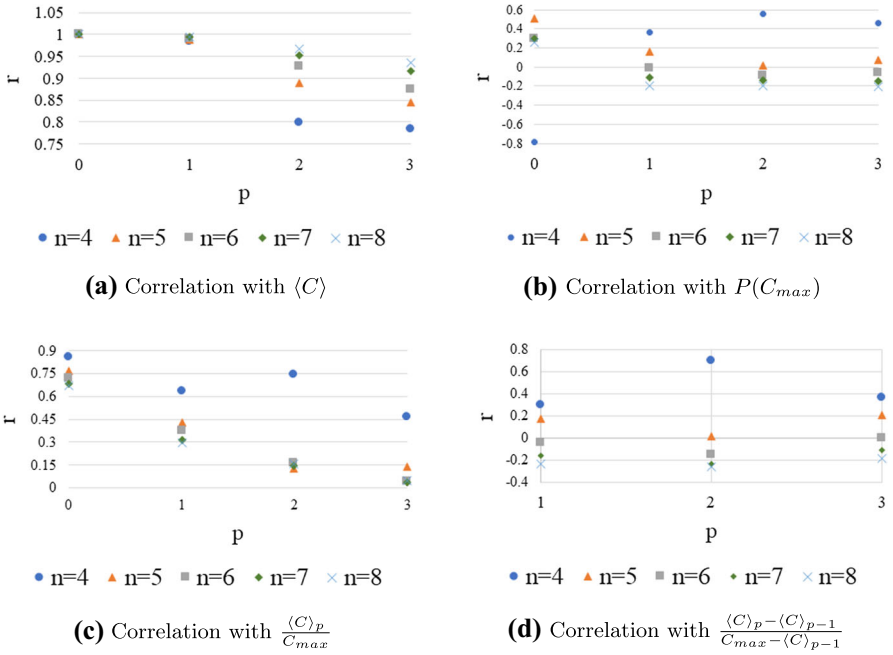

(a) Correlation with $\langle C \rangle$

(b) Correlation with $P(C_{max})$

(c) Correlation with $\frac{\langle C \rangle_p}{C_{max}}$

(d) Correlation with $\frac{\langle C \rangle_p - \langle C \rangle_{p-1}}{C_{max} - \langle C \rangle_{p-1}}$

Fig. 2 The correlations between the number of edges for each n vertex graph and each of the QAOA metrics for p

and their correlations with different QAOA metrics. Throughout each section, we will focus on the behavior of r as n and p increase, as these are small graphs that would not be representative of interesting problems that can provide a quantum advantage. Additionally, there are few graphs on four and five vertices compared to $n \in \{6, 7, 8\}$, so data points for $n \in \{4, 5\}$ may not be representative of the trends in correlations. Thus, we will focus our analysis on $n \geq 6$.

3.1 Edges, clique number, and minimal odd cycles

The correlation between number of edges and the metrics computed varies greatly. There is a very strong correlation between the number of edges and $\langle C \rangle$, which can be seen in Figs. 1 and 2a. This makes intuitive sense for the following reason. Arbitrarily adding edges to a given graph will not decrease the objective value of any given solution, only potentially increase it, so we would expect that denser graphs will have higher $\langle C \rangle$ values. However, the results in Fig. 2b show that the number of edges is negatively correlated with the probability of sampling an optimal solution for large n and p. We believe this is in part because the more edges that are added in a graph, the more near-optimal solutions there are that QAOA may favor over the optimal solution. These near-optimal solutions compete with exact optimal solutions in sampling, as QAOA optimizes $\langle C \rangle$, it can favor near-optimal states over truly optimal ones.

Note that as n increases, the correlation coefficient between edges and $\langle C \rangle$ increases toward 1 for fixed p, while the coefficients with $P(C_{\max})$, the approximation ratio, and the Δ ratio slightly decrease, as seen in Fig. 2. It is unclear why the size of n

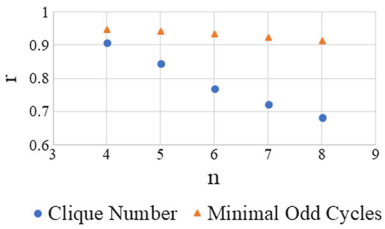

Fig. 3 The correlation coefficients of number of edges with clique number and number of minimal odd cycles

impacts the correlation coefficient. At large p, we expect that $\langle C \rangle$ would take the value of $C_{\max}$, so eventually, all of the approximation ratios will reach one, making them independent of the number of edges. The negative correlation in the change in approximation ratios can be explained as follows. As previously mentioned, denser graphs have high $\langle C \rangle$ and thus tend to have good approximation ratios. Hence, there is less room for improvement, whereas sparser graphs have more. We expect that for a fixed $n \geq 6$, Δ will approach zero as the number of iterations increases, as shown in Fig. 2d. The correlation is determined by the values of Δ and the fluctuations in Δ between graphs with various numbers of edges. When Δ becomes small, the fluctuations between graphs overwhelm the typical variations in Δ with the number of edges, so the correlation tends to zero.

Since the edge density, clique number, and number of minimal odd cycles are correlated for small n, as seen in Fig. 3, it is no surprise that they have strong correlations with the same QAOA metrics. Refer to Tables 4, 5, 6, and 7 to view their correlation coefficients. The properties become less correlated as n increases so it is unclear whether the properties will have similar r values for higher vertex graphs. The properties may need separate analyses for larger graphs. It could be that even though the properties become less correlated with each other, they remain highly correlated with some of the QAOA metrics.

In summary, the highest correlation between edges and the QAOA metrics is with $\langle C \rangle$. Thus, if a high expected value is the desired metric for success, graphs that are dense are optimal for QAOA. Edge density does not appear to have a large impact on $P(C_{\max})$ and the approximation ratio; however, simulations of larger graphs are needed to determine whether the correlations between edges and these metrics tend toward a limit between zero and negative one, or instead continue toward it. If the limit approaches negative one, then graphs with low edge density may yield higher probabilities of measuring an optimal solution or obtaining a high approximation ratio.

3.2 Diameter and number of cut vertices

For the most part, the diameter of a graph, d, correlates negatively with the QAOA metrics, but the correlation becomes less negative as n increases, which is the reverse of the correlations with the number of edges. The correlation is particularly strong with $\langle C \rangle$ for low values of p, as seen in Fig. 4a. This is not unexpected as diameter is negatively correlated with edge density. As seen in Fig. 4b, the correlation between diameter and probability of measuring an optimal state is stronger for smaller n and tends to approach zero for fixed n as p increases. Similarly to the probability, the

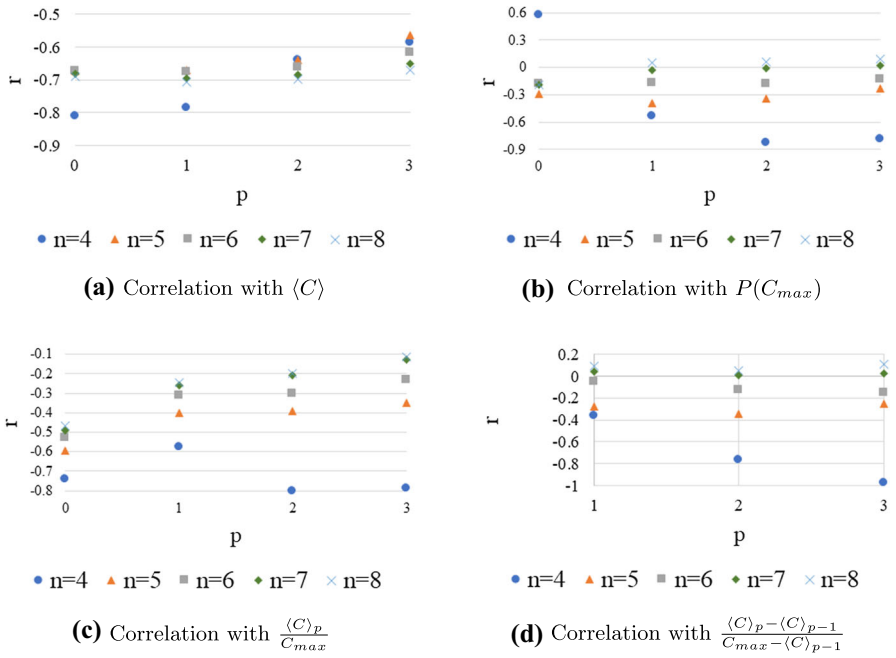

(a) Correlation with $\langle C \rangle$

(b) Correlation with $P(C_{max})$

(c) Correlation with $\frac{\langle C \rangle_p}{C_{max}}$

(d) Correlation with $\frac{\langle C \rangle_p - \langle C \rangle_{p-1}}{C_{max} - \langle C \rangle_{p-1}}$

Fig. 4 The correlations between the diameter for each n vertex graph and each of the QAOA metrics for p

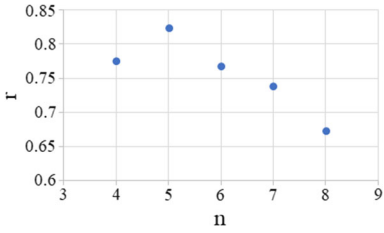

Fig. 5 The correlation coefficients between diameter and number of cut vertices for graphs on n vertices

correlation between d and the approximation ratio is stronger for smaller n and tends to approach zero for fixed n as p increases, as does the correlation between d and the Δ ratio. This is seen in Fig. 4c, d.

The number of cut vertices, like the diameter, correlates negatively with QAOA metrics, which makes sense as the two properties are positively correlated, as seen in Fig. 5; however, the correlation weakens as n increases. Thus, the two quantities may not correlate similarly with all of the QAOA metrics for larger n. See Tables 4, 5, 6, and 7 to see how the correlation coefficients compare between diameter and number of cut vertices.

As n increases, the correlation coefficient between diameter and $\langle C \rangle$ decreases as p increases, while the other metrics tend to increase, as seen in Fig. 4. In fact, the correlation with the other metrics approaches zero for high n and p. If these trends continue for $n \geq 9$, it would imply that diameter is not indicative of the success QAOA has when solving a MaxCut problem.

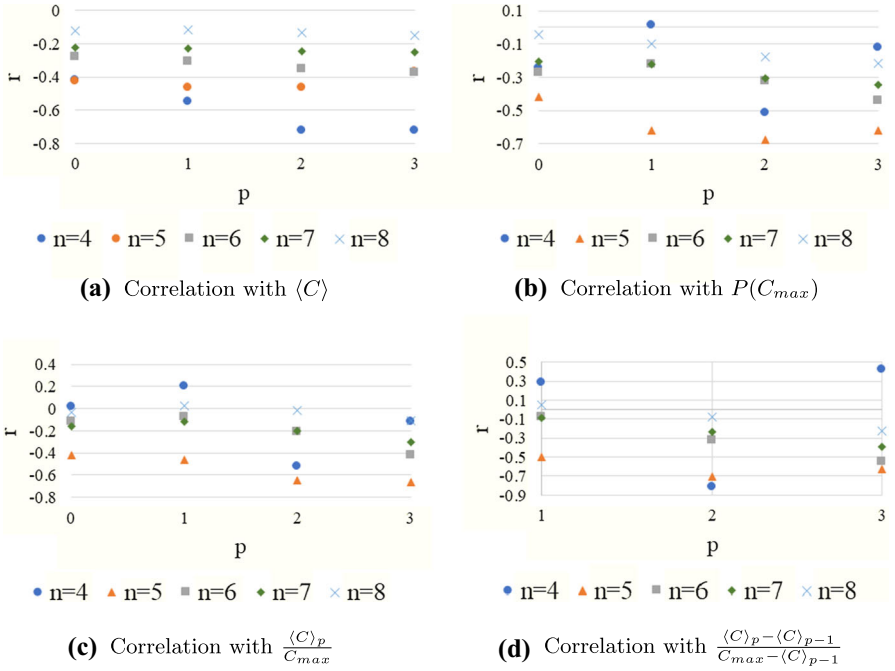

(a) Correlation with $\langle C \rangle$ **(b)** Correlation with $P(C_{max})$

(c) Correlation with $\frac{\langle C \rangle_p}{C_{max}}$ **(d)** Correlation with $\frac{\langle C \rangle_p - \langle C \rangle_{p-1}}{C_{max} - \langle C \rangle_{p-1}}$

Fig. 6 The correlations between the number of orbits for each n vertex graph and each of the QAOA metrics for p

3.3 Group size

The group size of a graph tends to have high positive correlations with all QAOA properties for small n. However as n increases, the correlations tend to zero. A zero correlation, however, might not indicate that the two are unrelated in this case. The size of the symmetry groups ranges from 1 to 2^n for all graphs on n vertices. Correlations are intended to measure linear relationships, so using data that is scaled exponentially on n could "wash out" the correlations. Instead of group size, we look at the number or orbits to better investigate the relationship between symmetry and QAOA performance.

3.4 Number of orbits

An automorphism of a graph is a relabeling of vertices that preserves edges and therefore is a type of symmetry. An orbit of a vertex v is the set of vertices with which v can be swapped in an automorphism. Thus, if there are two vertices in the same orbit but in different sets of an optimal MaxCut solution, there is a possibility that they can be swapped to give another optimal solution. If there are fewer large orbits, there are more possible symmetries than with many small orbits.

All vertices in the same orbit have the same degree, else the edges cannot be preserved. If there are more orbits, there are fewer symmetries, as there are fewer potential vertex mappings that preserve edges. It is not obvious why fewer orbits tend to produce better expected values and better approximation ratios. In Fig. 6a–d, we

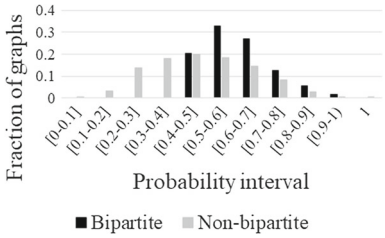

Fig. 7 The fraction of eight vertex bipartite and non-bipartite graphs with a given probability of finding an optimal solution for $p = 3$

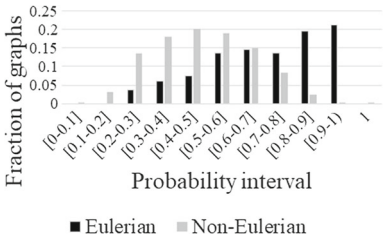

Fig. 8 The fraction of eight vertex Eulerian and non-Eulerian graphs with a given probability of finding an optimal solution for $p = 3$

see that, upon discarding $n = 4$, the correlation coefficient between number of orbits and the QAOA metrics tends to increase as n increases. Additionally, the correlation coefficient with the approximation ratio becomes more negative as p increases. Hence, graphs with small group sizes and larger orbits should achieve higher approximation ratios after several iterations of QAOA. Thus, group size and symmetry should play an important role in the quality of solution, which has been noted by Shaydulin, Hadfield, Hogg, and Safro [19].

3.5 Bipartite

Since there are so few bipartite graphs compared to non-bipartite for fixed n, looking at the average of each QAOA metric offers more insight into how a graph being bipartite affects the quality of QAOA solution. The average for all QAOA metrics are lower for bipartite graphs than non-bipartite when $p = 1$ for fixed n; however, the probability and change in approximation ratio are higher for bipartite graphs for larger p as seen in Table 8 and Fig. 7. Depending on the preferred metric of success, bipartite graphs either perform worse than non-bipartite, as in the case for the approximation ratio and $\langle C \rangle$, or better, as in the case of probability of measuring an optimal solution or Δ ratio. The average Δ ratio being higher for bipartite graphs suggests that a low approximation ratio at $p = 1$ does not imply that the approximation ratio at larger iterations cannot surpass those of non-bipartite graphs. The fact that the approximation ratio tends to be lower for bipartite graphs agrees with previous literature [4]. In fact, Wurtz and Love conjecture that for p iterations of QAOA on any graph, the approximation ratio of an n vertex graph is lower when there are no odd cycles of length at most $2p + 1$ than graphs that have length at most $2p + 1$ [20].

3.6 Eulerian

There are so few Eulerian graphs in the data set that the correlation coefficients are not particularly helpful; however, plotting the performance of Eulerian graphs makes

the relationship between them and the QAOA metrics more evident. As seen in Table 9, the average maximum probability, level p approximation ratio, and Δ ratios are significantly higher for Eulerian graphs than for non-Eulerian for most n and p, while the averages are comparable for the expected value of C. Figure 8 shows a histogram of the number of Eulerian and non-Eulerian graphs on eight vertices and the probability of obtaining an optimal solution. As seen in the histogram, for any given graph, the probability of measuring an optimal MaxCut solution is higher for Eulerian graphs than non-Eulerian.

3.7 Distance regular

Similarly to Eulerian graphs, distance regularity does not appear to have a strong correlation with any of the QAOA metrics because there are so few distance regular graphs compared to non-distance regular ones, so we do not make a chart of the correlations. In particular, there are only ten distance regular graphs on fewer than seven vertices. We also do not make a histogram with the probabilities as we did for Eulerian and bipartite graphs because the average probability of measuring an optimal solution for only a handful of distance regular graphs cannot be compared as well to the average probability of thousands of non-distance regular graphs. However, graphs with $n \in \{4, 5\}$ vertices that are distance regular have a probability of one of obtaining the optimal solution when $p = 2$. These graphs in particular are C_4, K_4, C_5 and K_5, where C_n denotes the cycle on n vertices and K_m denotes the complete graph on m vertices. These are the only distance regular graphs on four or five vertices, up to isomorphism. Interestingly enough, when $n = 7$, both distance regular graphs, C_7 and K_7, obtain a probability of one of being in the optimal state when $p = 3$; however, this is not the case for $n = 6$. When $n = 6$, three of the four distance regular graphs have a probability greater than 0.99 of giving the correct solution; however, the complete bipartite graph with partitions both containing three vertices ($K_{3,3}$) achieves a probability of 0.97. This is far higher than the average for arbitrary graphs with $n = 6$ and $p = 3$. These results lead us to believe that distance regular graphs on n vertices achieve a high probability of obtaining the optimal solution when $p \geq \lfloor \frac{n}{2} \rfloor$; however, more testing and a rigorous mathematical proof would be needed to confirm this.

4 Conclusion

The quantum approximate optimization algorithm has been studied in detail for the MaxCut problem on graphs with rigid structures including degree regularity and whether or not a graph is bipartite [3,8–10]. While the studies give insight into how the algorithm works, examining graphs with specific structures excludes the vast majority of graphs. Thus, we looked at properties of all connected graphs on at most eight vertices and found the correlation between different graph properties and the probability of finding an optimal solution, the expected value of C, the level p approximation ratio, and the change in ratio from $p - 1$ to p for p at most three.

Table 3 A summary of graph properties and average correlation coefficient over all $p \geq 1$ to QAOA metrics for $n = 8$

Graph Property	$\langle C \rangle$	$P(C_{max})$	$\frac{\langle C \rangle_p}{C_{max}}$	$\frac{\langle C \rangle_p - \langle C \rangle_{p-1}}{C_{max} - \langle C \rangle_{p-1}}$
Edges	+	−	+	−
Diameter	−		−	
Clique number	+	−	+	−
Bipartite	+		+	
Eulerian		−		−
Distance regular				
Number of cut vertices	−			
Number of minimal odd cycles	+	−	+	−
Group size				
Number of orbits	−	−		

A "+" means a strong positive average coefficient, "−" represents a strong average negative correlation coefficient, and an empty space means the average correlation coefficient is in the interval $(-.1, .1)$, which is not significant

There are two metrics that strongly correspond with the graph properties studied, namely $\langle C \rangle$ and $P(C_{\max})$. Graphs that have a lot of edges have a high positive correlation with $\langle C \rangle$. Diameter, clique size, number of cut vertices, and number of small odd cycles also correlate with $\langle C \rangle$, either positively or negatively. This is expected because these properties correlate positively or negatively with the number of edges for small n. Trends in the data for fixed n and increasing p are summarized in Table 2. The probability of measuring the optimal solution, expected value of C, and optimal angles was taken from [14,17].

Bipartite, Eulerian, and distance regular graphs tend to have higher probabilities of measuring the optimal solution than graphs that do not have any of these properties. For bipartite, this occurs for $p \geq 2$. Previous work shows that the approximation ratio for bipartite graphs tends to be worse than non-bipartite [4], so depending on the metric of success, bipartite graphs may or may not be suitable graphs for testing. Similarly, for larger p, Eulerian and distance regular graphs tend to have higher probabilities of measuring the optimal solution than non-Eulerian and non-distance regular graphs. Thus, we expect that QAOA for MaxCut on highly symmetric graphs, which are those with larger orbits, bipartite, Eulerian, and distance regular graphs will have a relatively high probability of measuring the optimal solution. Table 3 gives a summary of the average correlation coefficient over all $p \geq 1$ for each graph property and each QAOA metric on graphs with eight vertices.

Additionally, we created a data set containing the graphs and their properties. The data set information is located in Appendix 2. For future work, a similar data set for other problems, such as maximum independent set or problems with low circuit depth [21], would be useful to create benchmarks for experiments on NISQ devices. Other avenues of future work include using machine learning to determine whether MaxCut on a graph will have a high probability of measuring the optimal solution after p rounds of QAOA. Mathematically proving if QAOA for MaxCut on distance regular

graphs with n vertices gives better solutions than non-distance regular graphs after $\lfloor \frac{n}{2} \rfloor$ iterations would be of interest, as well.

Acknowledgements The authors would like to thank Ryan Bennink for his helpful comments on early drafts of this manuscript. This work was supported by DARPA ONISQ program under Award W911NF-20-2-0051. J. Ostrowski acknowledges the Air Force Office of Scientific Research Award, AF-FA9550-19-1-0147. G. Siopsis acknowledges the Army Research Office Award W911NF-19-1-0397. J. Ostrowski and G. Siopsis acknowledge the National Science Foundation Award OMA-1937008. This manuscript has been authored by UT-Battelle, LLC under Contract No. DE-AC05-00OR22725 with the US Department of Energy. The United States Government retains and the publisher, by accepting the article for publication, acknowledges that the United States Government retains a non-exclusive, paid-up, irrevocable, world-wide license to publish or reproduce the published form of this manuscript, or allow others to do so, for United States Government purposes. The Department of Energy will provide public access to these results of federally sponsored research in accordance with the DOE Public Access Plan. (http://energy.gov/downloads/doe-public-access-plan).

Appendix

Appendix A: graph theory definitions

In this section, we define some of the less common graph theory terms that appear in the paper.

Definition A.1 (*Diameter)* The diameter of a graph $G = (V, E)$ is $\max_{u,v} d(u, v)$, where $d(u, v)$ denotes the distance between $u, v \in V$.

Definition A.2 (*Distance)* The distance between two vertices, u and v, of a graph $G = (V, E)$ is the number of edges in the shortest path between u and v.

Definition A.3 (*Clique number)* The clique number of a graph is the size of the largest complete subgraph.

Definition A.4 (*Bipartite)* A graph is bipartite if the vertices can be partitioned into two sets such that all edges are incident to a vertex in both sets.

Definition A.5 (*Eulerian cycle)* An Eulerian cycle is a cycle that uses all edges of a graph exactly once.

Definition A.6 (*Eulerian)* A graph is Eulerian if it is connected and contains an Eulerian cycle.

Definition A.7 (*Distance Regular)* A graph $G = (V, E)$ is distance regular if for any pair of vertices $x, y \in V$, the number of vertices that are distance i from x equals the number of vertices that are distance i from y, for $i \in \{1, 2, ..., d\}$, where d is the diameter of G.

Definition A.8 (*Cut vertex)* A cut vertex of a connected graph is a vertex whose removal disconnects the graph.

Definition A.9 (*Graph Automorphism)* A graph automorphism is a relabeling of vertices that preserves the set of edges. Mathematically, it is a map $\alpha : V \longrightarrow V$ such that $ij \in E$ if and only if $\alpha(i)\alpha(j) \in E$.

Definition A.10 (*Automorphism Group)* The set of all graph automorphisms of G forms an automorphism group of G.

Definition A.11 (*Group Size)* The group size of G is the size of the automorphism group of G.

Definition A.12 (*Orbit)* An orbit of a vertex v is the set of all vertices $\alpha(v)$ where α is an automorphism of G.

Appendix B: database details

The data generated from these studies are shared in a publicly accessible GitHub Repository to serve as a benchmark QAOA calculations and experiments. This data set consists of csv files for each set of graphs on n vertices for $3 \leq n \leq 8$. The generated graph entries, which populate each set, are indexed by a graph number and include the following properties: bipartite (Boolean), number of edges, diameter, clique number, distance regular (Boolean), Eulerian (Boolean), list of cut vertices, number of cut vertices, cycle basis, degree sequence, automorphism group generator, automorphism group size, orbits, number of orbits, and the number of small cycles on 3 to n vertices. In addition to the data set, we have provided two options for storing and sorting this data by desired graph properties. The first option is to insert the data into a MySQL database structure. The user can then query the database to select the desired data and insert new columns for additional properties, calculations, and experimental results. We have provided scripts for creating the database tables, populating the tables using the csv files, querying the database, and inserting new columns. For additional information on how to download and use MySQL, see the MySQL Documentation.To work with the data set directly, we have also included a Python script which utilizes the data analysis library *pandas*. Pandas is a library which allows the user to store and manipulate data in two-dimensional, labeled data structures called DataFrames. We have provided a Python script which allows the user to import the csv data into pandas DataFrames and create new DataFrames with the desired graph properties. For more information on how to use and install pandas, see the Pandas Documentation. Both MySQL and Pandas are free, open-source software packages. This data set, the MySQL Scripts, and Python script can be accessed through the QAOA Small Graph GitHub Repository.

Appendix C: data tables

In this section, we include the tables containing all correlations between different graph properties and metrics. For the Boolean properties, we assign "1" to TRUE and "0" to FALSE. See Tables 4, 5, 6, 7, 8, and 9.

Table 4 The Pearson product–moment correlation between the probability of getting an optimal solution with p iterations of QAOA on an n vertex graph with the graph properties in columns two through eleven

n:p	Edges	Diam.	Clique num.	Bipartite	Eulerian	Dist. reg.	Num. cut vertices	Num. min. odd cycles	Grp. size	Num. orbits
4:0	−.781	.577	−.894	−1	−.447	0	.447	−.866	−.307	−.243
4:1	.363	−.535	.558	.398	.030	.437	−.085	.346	.507	.015
4:2	.561	−.830	.421	.247	−.512	.809	−.769	.354	.663	−.513
4:3	.462	−.786	.386	.410	−.222	.352	−.772	.355	.359	−.121
5:0	.505	−.287	.444	−.141	−.214	.450	−.152	.479	.767	−.417
5:1	.166	−.387	.243	.238	−.662	.661	−.110	.217	.531	−.619
5:2	.018	−.339	−.016	.047	−.447	.441	−.128	.004	.411	−.675
5:3	.071	−.233	.040	−.027	−.371	.277	−.127	.056	.296	−.619
6:0	.300	−.177	.209	−.027	−.371	.155	−.147	.301	.191	−.271
6:1	−.016	−.170	.043	.112	−.301	.222	.011	.012	.232	−.221
6:2	−.094	−.183	−.123	−.069	−.281	.252	.011	−.148	.272	−.324
6:3	−.059	−.131	−.126	−.153	−.271	.263	−.031	−.147	.209	−.441
7:0	.297	−.189	.287	.007	−.220	.015	−.133	.326	.043	−.208
7:1	−.110	−.027	−.037	.050	−.354	.216	.052	−.058	.202	−.224
7:2	−.140	−.012	−.167	−.058	−.298	.150	.053	−.158	.148	−.309
7:3	−.145	.024	−.207	−.100	−.252	.101	.066	−.201	.104	−.344
8:0	.256	−.192	.239	.028	−.131	.003	−.115	.286	.015	−.045
8:1	−.198	.056	−.124	.009	−.198	.029	.067	−.158	.056	−.101
8:2	−.194	.062	−.210	−.061	−.191	.047	.066	−.223	.057	−.178
8:3	−.201	.094	−.237	−.092	−.169	.046	.078	−.258	.040	−.214

Table 5 The Pearson product–moment correlation between $\langle C \rangle_p$ for an n vertex graph with the graph properties in columns two through eleven

n:p	Edges	Diam.	Clique num.	Bipartite	Eulerian	Dist. reg.	Num. cut vertices	Num. min. odd cycles	Grp. size	Num. orbits
4:0	1	−.812	.908	.781	.070	.552	−.768	.947	.746	−.417
4:1	.983	−.786	.824	.672	−.101	.669	−.819	.876	.761	−.548
4:2	.799	−.639	.479	.355	−.481	.761	−.920	.583	.608	−.725
4:3	.783	−.586	.450	.338	−.448	.709	−.901	.579	.572	−.725
5:0	1	−.673	.845	.558	−.247	.267	−.691	.951	.527	−.424
5:1	.989	−.671	.774	.495	−.255	.305	−.739	.908	.527	−.464
5:2	.889	−.641	.571	.256	−.118	.180	−.781	.730	.456	−.463
5:3	.844	−.564	.514	.234	−.087	.072	−.757	.679	.353	−.369
6:0	1	−.673	.768	.466	−.052	.189	−.684	.933	.323	−.277
6:1	.991	−.676	.697	.401	−.073	.221	−.729	.886	.319	−.305
6:2	.926	−.662	.544	.250	−.087	.256	−.750	.749	.312	−.351
6:3	.875	−.618	.468	.178	−.098	.264	−.747	.676	.274	−.372
7:0	1	−.683	.722	.329	−.079	.056	−.655	.924	.147	−.225
7:1	.994	−.695	.663	.295	−.081	.057	−.698	.884	.142	−.227
7:2	.953	−.684	.558	.214	−.074	.044	−.711	.790	.132	−.245
7:3	.916	−.651	.500	.169	−.067	.030	−.697	.731	.116	−.252
8:0	1	−.691	.682	.222	−.021	.024	−.603	.913	.050	−.123
8:1	.995	−.707	.629	.203	−.024	.028	−.646	.876	.048	−.117
8:2	.967	−.698	.550	.158	−.026	.034	−.652	.803	.046	−.136
8:3	.936	−.671	.507	.125	−.028	.040	−.640	.752	.042	−.153

Table 6 The Pearson product–moment correlation between the level p approximation ratio on an n vertex graph with the graph properties in columns two through eleven

n:p	Edges	Diam.	Clique num.	Bipartite	Eulerian	Dist. reg.	Num. cut vertices	Num. min. odd cycles	Grp. size	Num. orbits
4:0	.857	−.740	.988	.926	.414	.252	−.446	.926	.602	.017
4:1	.635	−.576	.886	.819	.515	.125	−.133	.753	.491	.206
4:2	.747	−.800	.552	.440	−.512	.810	−.882	.525	.630	−.520
4:3	.466	−.785	.389	.416	−.219	.347	−.777	.360	.356	−.119
5:0	.770	−.592	.856	.744	−.414	.389	−.397	.849	.499	−.421
5:1	.428	−.400	.569	.599	−.510	.549	−.164	.546	.421	−.463
5:2	.125	−.390	.152	.091	−.335	.483	−.154	.147	.424	−.648
5:3	.138	−.350	.103	.060	−.373	.318	−.206	.116	.329	−.666
6:0	.720	−.530	.800	.681	−.040	.061	−.350	.822	.246	−.116
6:1	.374	−.314	.539	.541	−.066	.051	−.103	.515	.192	−.071
6:2	.166	−.300	.218	.234	−.133	.140	−.050	.193	.258	−.212
6:3	.042	−.231	−.035	−.057	−.256	.298	−.099	−.033	.234	−.420
7:0	.687	−.489	.727	.494	−.120	.074	−.337	.794	.127	−.158
7:1	.315	−.258	.442	.387	−.140	.112	−.113	.462	.107	−.116
7:2	.143	−.210	.182	.207	−.164	.134	−.063	.206	.130	−.202
7:3	.035	−.128	−.015	.028	−.182	.117	−.023	.010	.112	−.305
8:0	.671	−.469	.666	.347	−.032	−.007	−.314	.778	.039	−.034
8:1	.299	−.247	.383	.276	−.042	−.009	−.129	.443	.031	.024
8:2	.157	−.197	.163	.175	−.063	.004	−.082	.227	.037	−.015
8:3	.051	−.115	−.002	.043	−.090	.031	−.037	.043	.039	−.107

Table 7 The Pearson product–moment correlation between the Δ ratio at p on an n vertex graph with the graph properties in columns two through eleven

n:p	Edges	Diam.	Clique num.	Bipartite	Eulerian	Dist. reg.	Num. cut vertices	Num. min. odd cycles	Grp. size	Num. orbits
4:1	.295	−.362	.619	.513	.451	.079	.192	.418	.368	.288
4:2	.701	−.766	.412	.192	−.567	.897	−.901	.465	.742	−.809
4:3	.362	−.979	.483	.483	NA	NA	−.682	.362	.511	.422
5:1	.175	−.276	.305	.306	−.612	.645	−.001	.271	.487	−.495
5:2	.015	−.347	−.045	−.140	−.490	.571	−.140	−.011	.507	−.710
5:3	.204	−.251	.177	.095	−.423	NA	−.114	.158	.700	−.623
6:1	−.045	−.053	.139	.209	−.110	.112	.149	.077	.200	−.078
6:2	−.153	−.124	−.240	−.203	−.228	.310	.045	−.252	.395	−.318
6:3	−.003	−.152	−.139	−.206	−.393	.438	−.099	−.119	.337	−.545
7:1	−.157	.045	.018	.122	−.182	.180	.148	−.025	.160	−.090
7:2	−.235	.012	−.324	−.146	−.244	.226	.080	−.315	.235	−.237
7:3	−.114	.029	−.210	−.159	−.308	.211	.069	−.208	.176	−.392
8:1	−.237	.090	−.078	.078	−.057	.007	.124	−.104	.041	.053
8:2	−.259	.048	−.389	−.091	−.102	.045	.077	−.361	.079	−.077
8:3	−.187	.107	−.279	−.159	−.166	.082	.088	−.302	.083	−.226

Table 8 The average value of bipartite graphs versus non-bipartite graphs, where the columns beginning with "B." refer to bipartite graphs and those with "N.B." refer to non-bipartite graphs

n:p	B. $P(C_{max})$	N.B. $P(C_{max})$	B. $\langle C \rangle$	N.B.$\langle C \rangle$	B. Level p A.R.	N.B. Level p A.R.	B. Δ ratio $p-1$ to p	N.B. Δ ratio $p-1$ to p
4:0	.125	.0625	1.667	2.5	.5	.681	NA	NA
4:1	.481	.602	2.566	3.216	.772	.879	.544	.634
4:2	.889	.928	3.180	3.586	.949	.978	.762	.825
4:3	.993	.999	3.326	3.666	.998	1.000	.973	.994
5:0	.0625	.049	2.3	3.344	.5	.658	NA	NA
5:1	.368	.495	3.436	4.323	.750	.857	.500	.605
5:2	.746	.725	4.222	4.685	.918	.928	.661	.587
5:3	.907	.900	4.470	4.926	.970	.974	.731	.744
6:0	.031	.028	3.118	4.447	0.500	0.644	NA	NA
6:1	.260	.311	4.542	5.672	.733	.826	.465	.522
6:2	.586	.549	5.449	6.179	.873	.900	.519	.442
6:3	.818	.744	5.949	6.506	.951	.946	.620	.511
7:0	.016	.016	3.875	5.693	.067	.074	NA	NA
7:1	.182	.213	5.554	7.187	.438	.482	.182	.213
7:2	.469	.424	6.598	7.827	.851	.886	.464	.396
7:3	.691	.605	7.201	8.225	.927	.930	.519	.409
8:0	.008	.011	4.797	7.246	.5	.646	NA	NA
8:1	.133	.139	6.773	9.022	.710	.808	.420	.462
8:2	.385	.317	7.983	9.801	.832	.877	.420	.367
8:3	.606	.482	8.762	10.273	.911	.920	.467	.350

The abbreviation "A.R.' stands for the approximation ratio. Three vertex graphs are excluded since there is one bipartite three vertex graph and one non-bipartite

Table 9 The average value of Eulerian graphs versus non-Eulerian graphs, where the columns beginning with "E." refer to Eulerian graphs, and those with "N.E." refer to non-Eulerian graphs

$n{:}p$	E. $P(C_{max})$	N.E. $P(C_{max})$	E. $\langle C \rangle$	N.E. $\langle C \rangle$	E. Level p A.R.	N.E. Level p A.R.	E. Δ ratio $p-1$ to p	N.E. Δ ratio $p-1$ to p
4:0	.125	.088	2	2.1	.5	.608	NA	NA
4:1	.531	.543	3.000	2.869	.75	.841	.5	.607
4:2	1	.890	4	3.260	1	.956	1	.752
4:3	1	.995	4	3.395	1	.998	1	.980
5:0	.070	.048	3.5	3	.698	.602	NA	NA
5:1	.775	.392	4.513	4.017	.912	.813	.764	.537
5:2	.913	.687	4.762	4.531	.960	.918	.831	.551
5:3	.990	.881	4.965	4.782	.994	.968	.963	.689
6:0	.078	.025	4.438	4.231	.633	.621	NA	NA
6:1	.481	.290	5.766	5.480	.827	.811	.552	.510
6:2	.749	.539	6.397	6.043	.915	.894	.566	.445
6:3	.925	.742	6.816	6.391	.976	.945	.796	.507
7:0	.041	.015	6.054	5.578	.075	.074	NA	NA
7:1	.431	.201	7.570	7.081	.843	.807	.569	.475
7:2	.666	.415	8.203	7.744	.912	.883	.518	.394
7:3	.833	.600	8.597	8.153	.955	.929	.609	.406
8:0	.027	.011	7.438	7.202	.656	.643	NA	NA
8:1	.276	.137	9.245	8.981	.820	.806	.491	.461
8:2	.525	.315	10.067	9.766	.893	.876	.426	.366
8:3	.708	.480	10.580	10.242	.937	.919	.472	.350

The abbreviation "A.R." stands for the approximation ratio. Three vertex graphs are excluded since there is one Eulerian three vertex graph and one non-Eulerian. The entries for Eulerian 4:3 are the same as Eulerian 4:2 since the only Eulerian graph on four vertices achieves its maximum values after two iterations

References

1. Bravyi, S., Gosset, D., König, R.: Quantum advantage with shallow circuits. Science **362**(6412), 308–311 (2018)
2. Riste, D., da Silva, M.P., Ryan, C.A., Cross, A.W., Córcoles, A.D., Smolin, J.A., Gambetta, J.M., Chow, J.M., Johnson, B.R.: Demonstration of quantum advantage in machine learning. Quant. Inf. **3**(1), 1–5 (2017)
3. Farhi, E., Goldstone, J., Gutmann, S.: A quantum approximate optimization algorithm. arXiv preprint arXiv:1411.4028, (2014)
4. Farhi, E., Gamarnik, D., Gutmann, S.: The quantum approximate optimization algorithm needs to see the whole graph: Worst case examples. arXiv preprint arXiv:2005.08747, (2020)
5. Conforti, M., Cornuéjols, G., Zambelli, G., et al.: Integer programming. Springer, Berlin (2014)
6. Festa, P., Pardalos, P.M., Resende, M.G.C., Ribeiro, C.C.: Randomized heuristics for the MAX-CUT problem. Optim. Methods Softw. **17**(6), 1033–1058 (2002)
7. Goemans, M.X., Williamson, D.P: 879-approximation algorithms for max cut and max 2sat. In Proceedings of the twenty-sixth annual ACM symposium on theory of computing, pages 422–431, (1994)
8. Brandão, F. G. S. L., Broughton, M., Farhi, E., Gutmann, S., Neven, H.: For fixed control parameters the quantum approximate optimization algorithm's objective function value concentrates for typical instances. arXiv preprint arXiv:1812.04170, (2018)
9. Medvidović, M., Carleo, G.: Classical variational simulation of the quantum approximate optimization algorithm. arXiv preprint arXiv:2009:01760v1, (2020)
10. Zhou, L., Wang, S.-T., Choi, S., Pichler, H., Lukin, M. D.: Quantum approximate optimization algorithm: performance, mechanism, and implementation on near-term devices. arXiv preprint arXiv:1812.01041, (2018)
11. Akshay, V., Philathong, H., Zacharov, I., Biamonte, J.: Reachability deficits implicit in google's quantum approximate optimization of graph problems. arXiv preprint arXiv:2007.09148, (2020)
12. Farhi, E., Gamarnik, D., Gutmann, S.: The quantum approximate optimization algorithm needs to see the whole graph: a typical case. arXiv preprint arXiv:2004.09002, (2020)
13. Ozaeta, A., van Dam, W., McMahon, P. L.: Expectation values from the single-layer quantum approximate optimization algorithm on ising problems. arXiv preprint arXiv:2012.03421, (2020)
14. Lotshaw, P. C., Humble, T. S., Herrman, R., Ostrowski, J., Siopsis, G.: Empirical performance bounds for quantum approximate optimization. arXiv preprint arXiv:2102.06813, (2021)
15. Belotti, P.: Couenne: a user's manual. Technical report, Technical report, Lehigh University, (2009)
16. Press, W. H., Flannery, B. P., Teukolsky, S. A.: Numerical recipes in Fortran 77: the art of scientific computing. Cambridge University Press, second edition, (1993). https://people.sc.fsu.edu/~inavon/5420a/DFP.pdf
17. Lotshaw, P. C., Humble, T. S.: QAOA dataset. Found at https://code.ornl.gov/qci/qaoa-dataset-version1
18. McKay, B.: Graphs [data set]. Found at http://users.cecs.anu.edu.au/~bdm/data/graphs.html
19. Shaydulin, R., Hadfield, S., Hogg, T., Safro, I.: Classical symmetries and QAOA. arXiv preprint arXiv:2012.04713, (2020)
20. Wurtz, J., Love, P. J: Bounds on MAXCUT QAOA performance for p> 1. arXiv preprint arXiv:2010.11209, (2020)
21. Herrman, R., Ostrowski, J., Humble, T.S., Siopsis, G.: Lower bounds on circuit depth of the quantum approximate optimization algorithm. Quant. Inf. Process. **20**(59), 1 (2021)